Penerbit Akademia Baru

Malaysian Journal on Composites Science and Manufacturing

Journal homepage:
https://www.akademiabaru.com/submit/index.php/mjcsm/
ISSN: 2716-6945

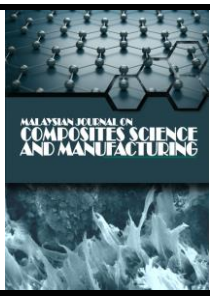

Numerical Analysis of Combustion and Emission Characteristics of a Diesel Engine Fueled with 40Butanol/60Diesel Blended Fuel

Open Access

Anik Biswas[1,*], Kazi Mostafijur Rahman[1]

[1] Department of Mechanical Engineering, Khulna University of Engineering & Technology, Khulna-9203 Bangladesh.

ARTICLE INFO

Article history:
Received 10 December 2023
Received in revised form 5 April 2024
Accepted 23 April 2024
Available online 30 July 2024

ABSTRACT

As the energy requirements of power-producing systems increase, fossil fuels are becoming rare worldwide. Diesel engines are a common and efficient source of power generation. Nonetheless, several national and international bodies impose restrictions on diesel engine emissions for environmental safety. So, to reduce harmful diesel engine emissions, some steps should be followed, including lowering emissions and increasing performance. Butanol is a well-known biofuel with comparatively lower emission characteristics and higher performance than diesel. Blending butanol with diesel can increase the performance and improve the emission characteristics of a diesel engine. This study introduces a 40% butanol: 60% diesel blend (D60B40) to a single-cylinder, four-stroke, direct-injection diesel engine to investigate the combustion properties and emission characteristics using ANSYS Forte software. Effects of different start of injection (SOI) of 30˚, 26˚, 22˚ and 18˚ Before Top Dead Center (BTDC) were studied. Results show that early injection leads to greater temperatures, pressures, and apparent heat release rates (AHRR), which all reduce carbon monoxide (CO) and unburned hydrocarbon (UHC) emissions but cost more Nitrogen Oxide (NOx) emissions. Combustion efficiency is 2.66% higher for 30˚ BTDC than 18˚ BTDC. Thermal efficiency shows a 0.2% increase for 18˚ BTDC due to low wall heat transfer loss. NOx emission is 2.983 g/kWh for 30˚ BTDC, whereas 18˚ BTDC had only 0.544 g/kWh. To reduce the NOx emission due to increasing blend ratio and advanced SOI, exhaust gas recirculation (EGR) is also investigated (0%, 10%, 20% & 30%) for D60B40 at 30˚ BTDC. At 30% EGR, the investigation reveals an improvement in emission characteristics, with NOx emission of 0.169 g/kWh, about 90.5% lower than D100. The CO emission increases from 1.485 g/kWh to 5.345 g/kWh, about 4 times more than 0% EGR. By using a higher butanol/diesel blend of D60B40 with early injection at 30˚ BTDC and an EGR rate of 30%, it is feasible to satisfy the standards of many national and international organizations and improve combustion performance.

Keywords:
N-Butanol, Diesel, Diesel engine, Injection timing, Exhaust gas recirculation, Combustion, Emission

[*] *Corresponding author.*
E-mail address: anikbiswas1705020@gmail.com (Anik Biswas)
E-mail of co-authors: mostafij@me.kuet.ac.bd

https://doi.org/10.37934/mjcsm.14.1.4457

1. Introduction

Internal combustion engines have contributed significantly to humanity's advancement. Despite their benefits, engines also provide several difficulties, including higher fuel costs and greater air pollution. This motivated the scientists to work on improved combustion techniques that might result in greater fuel efficiency and reduced emissions. Due to the growing ecological and environmental concerns about traditional fossil fuels and the strict restrictions governing exhaust emissions, the engine industry and vehicle manufacturers have given renewable energy more consideration for the next generation of engines [1,2]. The next generation of biofuels may be produced from renewable resources and agricultural waste products, such as cornstalks and wheat shafts, which provide the intriguing prospect and promise of renewability in that the biofuels may be fully restored by the environment and fully achieve a dynamic equilibrium between the carbon source and carbon sink by employing the combustion products of the fuels [3]. Butanol is a good fuel alternative that can be produced from biological waste products and is a renewable fuel source [4,5,6]. It is seen in experimental research that adding butanol with diesel and charging the mixture into the engine reduces CO emissions and increases the release of EINOx (EINOx stands for "Exhausted Inhibited Nitrous Oxide." EINOx is a chemical compound which is produced by the reaction of an NOx (Nitrogen Oxides) exhaust treatment additive with diesel engine exhaust gases). Also, the combustion characteristics improve with the increase of butanol percentage in the mixture. Luis *et al.* [7] studied the effects of butanol/diesel blends using 5%, 10% and 20% of butanol in the mixture. However, engine construction and other operating parameters, such as spray models and pressure, affect combustion and emission characteristics [8,9]. Injection timing is one such operating condition that plays a dominant role. Advancing or retarding the fuel injection time affects the combustion and emission characteristics [10].

There is an adverse effect of using butanol with diesel fuel. It increases the amount of NOx in the combustion products [11]. NOx is a harmful environmental product that must be reduced [12]. Investigations have found that using an exhaust gas recirculation system (EGR) reduces the amount of NOx emission significantly. With the increase of the EGR rate, the NOx emission is lower. Engine performance gets better [11,13,14].

This study was conducted to find out the outcomes when the percentage of butanol in the blend was 40%. Effects of injection timing (30˚,26˚,22˚,18˚ BTDC) are investigated, and finally, advanced SOI (30˚ BTDC) is selected for further analysis of the combustion and emission characteristics with EGR (0%, 10%, 20%, 30%).

2. Methodology

2.1 CFD Model & Ansys Forte

The ANSYS-developed FORTE 2022 R1 software was used to model the functioning of an IC engine. The software combines a highly effective and comprehensive pre-defined industry standard chemical kinetics (CHEMKIN files) that solves chemical reaction mechanisms and specifies thermodynamic data based on Arrhenius-type correlation with the CFD code, which was used to solve liquid spray, turbulent gas dynamics, and other transport equations. Figure 1 shows the flow of operations of ANSYS FORTE.

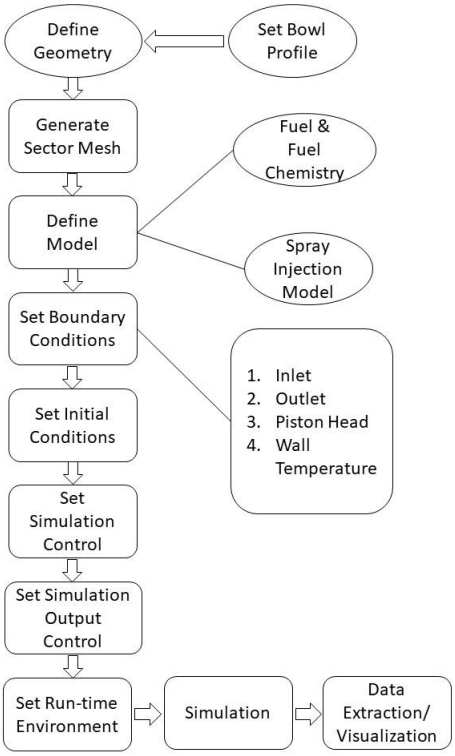

Fig. 1. Ansys Forte Simulation flow chart

2.2 Governing Equations

The air-fuel combination prior to combustion and the burnt by-products following combustion serve as the working fluids for internal combustion engines. The Navier Stokes Equation governs fundamental fluid dynamics in turbulent reacting flows, which are turbulent flows with chemical mixing and reactivity and were represented on ANSYS Forte.

Governing equations such as continuity, momentum, and energy equations were modified on the basis of Reynolds-averaged Navier-Stokes (RANS) equations. RANS was based on the semi-implicit method for pressure-linked equations and the k-ε standard turbulence model for numerical flow simulation [15,16].

2.2.1 Species Conservation Equation

Models of engine working fluids (gas phase) combine different gas species or gas component kinds. Due to interactions with fuel sprays, combustion, and molecular diffusion, the engine cycle alters each individual gas component. Let a species be *k*, and then the conservation equation (Eq. 1) is as follows:

$$\frac{\partial \bar{\rho}_k}{\partial t} + \nabla(\bar{\rho}_k \tilde{u}) = \nabla[\bar{\rho}_k D \bar{y}_k] + \nabla\varphi + \bar{\rho}_k^c + \bar{\rho}_k^s \quad (Here, k = 1,2,3, \dots K) \tag{1}$$

Here, ρ is the density, subscript k means species index, K is the total number of species, and u is the flow velocity vector.

The term φ (Eq. 2) accounts for the effects of the ensemble-averaging the convection term:

$$\varphi = \bar{\rho}_k \tilde{u} - \overline{\rho_k u} \tag{2}$$

$\bar{\rho}_k^C$ and $\bar{\rho}_k^S$ are terms due to chemical reactions and spray evaporation, respectively.

2.2.2 Fluid Continuity Equation

The continuity equation (Eq. 3) for the total gas phase fluid is:

$$\frac{\partial \bar{\rho}}{\partial t} + \nabla(\bar{\rho}\tilde{u}) = \overline{\rho^S} \tag{3}$$

2.2.3 Momentum Conservation Equation

The momentum equation (Eq. 4) is:

$$\frac{\partial \bar{\rho}\tilde{u}}{\partial t} + \nabla(\bar{\rho}\tilde{u}\tilde{u}) = -\nabla\bar{p} + \nabla\bar{\sigma} - \frac{2}{3}\bar{\rho}\tilde{k}I + \bar{F}^S + \bar{\rho}\bar{g} \tag{4}$$

Where, p is the pressure, $\bar{F}^S$ is the rate of momentum gain per unit volume due to the spray, $\bar{g}$ is the specific body force, $\bar{\sigma}$ is the viscous shear stress, $\bar{\sigma} = \bar{\rho}v\left[\nabla\tilde{u} + (\nabla\tilde{u})^T - \frac{2}{3}(\nabla\tilde{u})I\right]$, v is laminar kinetic velocity, I is the identity tensor, and superscript T means transpose of a tensor.

2.2.4 Energy Conservation Equation

The internal energy transport equation (Eq. 5) is:

$$\frac{\partial \bar{\rho}\tilde{I}}{\partial t} + \nabla(\bar{\rho}\,\widetilde{u}\tilde{I}) = -\bar{\rho}\nabla\widetilde{u} - \bar{p}\nabla\tilde{u} - \nabla\tilde{J} - \nabla H + \bar{\rho}\tilde{\varepsilon} + \bar{Q}^C + \bar{Q}^S \tag{5}$$

Where, I is the specific internal energy, J is the heat flux vector, $\tilde{J} = -\lambda\nabla\tilde{T} - \bar{\rho}D_T\sum_k \bar{h}_k\nabla\left(\frac{\bar{\rho}_k}{\rho}\right)$, λ is the thermal conductivity, which is related to the thermal diffusivity α and heat capacity C_p by $\lambda = \bar{\rho}C_p\alpha$, T is the temperature, $\bar{h}_k$ is the specific enthalpy of species k, and $\tilde{\varepsilon}$ is the dissipation rate due to chemical heat release and spray interactions, respectively.

2.2.5 RANS Equation

The Reynolds Average Navier-Stokes (RANS) is a time-averaged equation and can be expressed as in Eq. 6:

$$\frac{\partial(\rho u_i)}{\partial x_i} = 0$$
$$\frac{\partial(\rho u_i u_j)}{\partial x_j} = \frac{\partial p}{\partial x_i} + \frac{\partial}{\partial x_j}\left[\mu\left(\frac{\partial u_i}{\partial x_j} + \frac{\partial u_j}{\partial x_i} - \frac{2}{3}\delta_{ij}\frac{\partial u_l}{\partial x_l}\right)\right] + \frac{\partial}{\partial x_j}\left(-\rho\overline{u'_i u'_j}\right) \tag{6}$$

Here, u is the velocity of the fluid, ρ is the density of the fluid, and μ is the dynamic viscosity of the fluid.

2.3 Chemical Kinetics Formulation

The chemical reactions that occur in combustion simulations can be described by chemical kinetic mechanisms that define the reaction pathways and the associated reaction rates leading to the change in species concentrations. In detailed chemical kinetic mechanisms, the reversible or irreversible reactions involving k chemical species can be represented in the general form, Eq. 7:

$$\sum_{k=1}^{k} v' \, ki^{\chi}k \Leftrightarrow \sum_{k=1}^{k} v'' \, ki^{\chi}k \; (i1, \ldots, I) \tag{7}$$

The production rate of the k^{th} species in the *i*th reaction can be written as in Eq. 8:

$$\dot{\omega}_{ki} = (v''_{ki} - v'_{ki}) q_i (k = 1, \ldots, K) \tag{8}$$

Where q_i is the rate of progress of reaction *i* [17].

2.4 Engine Specifications

For this study, a Cummins N-14, single-cylinder, direct-injection diesel engine was used. It had two intake valves and a single exhaust valve. The combustion chamber was quiescent and used direct injection. The Bore diameter was 13.97 cm, and the height of the engine cylinder was 15.8 cm. Bowl width and depth were 9.05 cm and 1.346 cm, respectively. The length of the connecting rod was 30.48 cm. The nozzle had eight equally spaced holes with an orifice area of 0.00302 cm^2 each, and a common rail, a pilot valve, was used for actuated fuel injection. The compression ratio of the engine was 15. The injection pressure was 2.215 bar.

2.5 Boundary Conditions

The piston temperature was set to 500K, and the stroke length was set to 15.45 cm. The sector angle was 45°, the head temperature was 470K, and the liner temperature was 420K.

2.6 Geometry and Meshing

The geometry represents a section of the engine cylinder since the cylinder is symmetric. The sector angle in this simulation was 45°. The section was divided into 17619 sections. Mesh independency was checked for 1386, 8262, 15560, 17619, 21784 and 32671 cell numbers respectively.

Figure 2 shows the sector geometry and meshing. For mesh independency testing, maximum pressure and maximum temperatures were analyzed. Figure 3 shows the consistency of both pressure and temperature data after 17619 cell numbers.

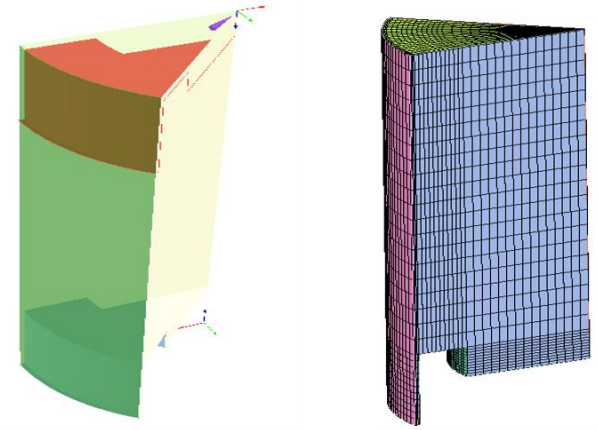

(a) (b)

Fig. 2. (a) Sector Geometry (b) Geometry Meshing

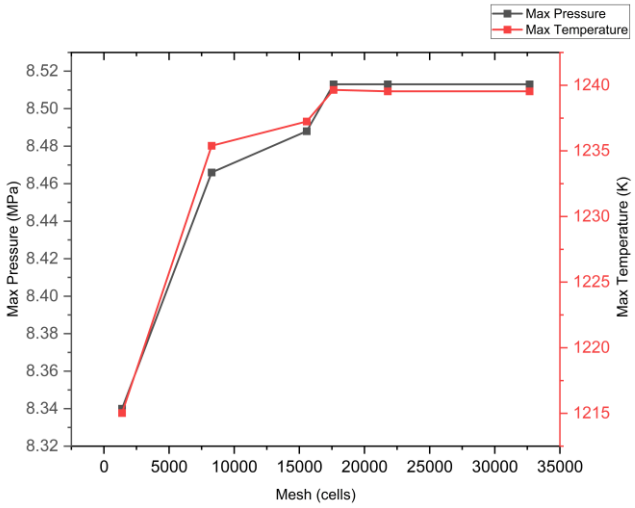

Fig. 3. Mesh Independency Test

3. Results

3.1 Injection Timing

The moment fuel is injected into the cylinder for the first time is known as the injection timing. This influences the time at which combustion occurs. A diesel's combustion, emission, and performance properties are all impacted by its presence. Improvements may be made to the characteristics for a more effective beginning to the injection process. Table 1 states the different start of injection (SOI) of fuel blend into the engine cylinder ranging from 30˚ to 18˚ BTDC for the mixture of 60% n-heptane and 40% n-butanol (D60B40).

Table 1
Parametric Study table for different SOI for D60B40

Serial	Start of Injection (BTDC)
1	SOI= 18
2	SOI= 22
3	SOI= 26
4	SOI= 30

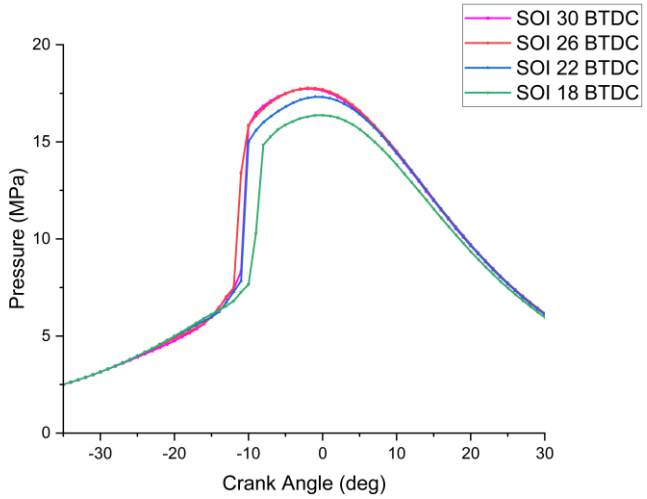

Fig. 4. In-cylinder Pressure distribution for 40% butanol blend (Pressure vs CA)

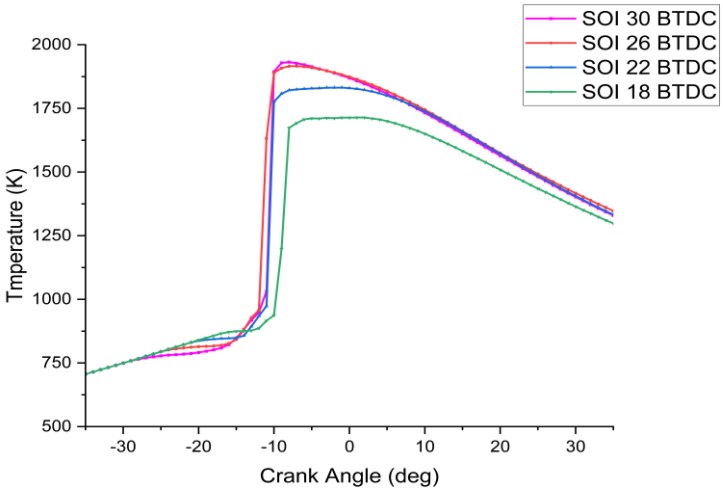

Fig. 5. In-cylinder Temperature distribution for 40% butanol blend (Temp. vs CA)

The Figure 4 shows the pressure distribution vs crank angle (CA) for a 40% butanol blend. The pressure distribution goes through a remarkable transformation from the beginning of the injection to its conclusion. The pressure and temperature of the cylinder are below the threshold required to begin the injection procedure at this earlier stage. As a result, there is an increase in the development of diesel and butanol mixed fuel when the ignition delay is in effect. The highest amount of ignition takes place at an SOI of 30˚ TDC (Top Dead Center). The air-fuel combination burns rapidly, which causes a rapid increase in pressure and temperature inside the cylinder. This is necessary to achieve

a longer ignition delay. When a large volume of fuel is burnt at a high heat release rate, a process known as premixed combustion takes place. This results in a shorter amount of time spent in the combustion stage.

In the case of temperature, the reduction is seen in Figure 5. When the injection timing is advanced, more fuel is collected if the ignition delay is left on for longer. A higher rate of heat production is achieved by the process of premixed combustion, which sees the burning of the bulk of the fuel. Because of this, advancing the injection time causes the temperature of the cylinder to rise. SOI= 30° BTDC shows maximum temperature meaning the injection is advanced at this point, while SOI= 18° BTDC shows lowest temperature rise meaning retarded injection.

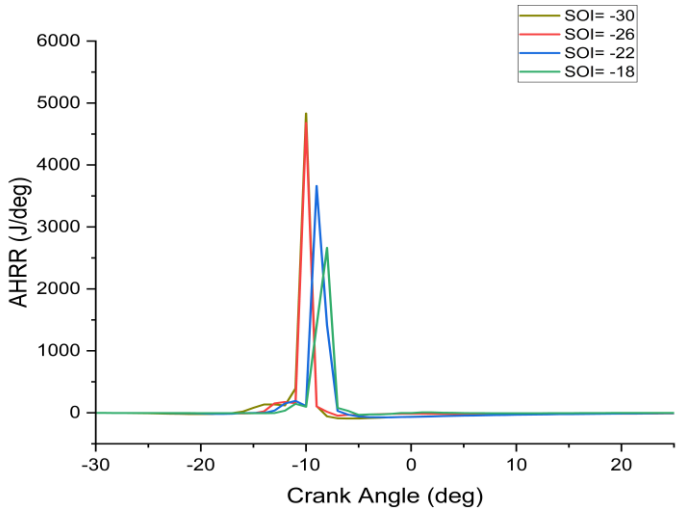

Fig. 6. AHRR distribution for 40% butanol blend (AHRR vs CA)

Figure 6 represents the distribution of apparent heat release rate (AHRR) with respect to injection timing (SOI) changes. It shows the gradual decrease in apparent heat release rate when the injection time is retarded. When the injection time was delayed, the cylinder's temperature and pressure increased to potentially hazardous levels just before the injection occurred. When high temperatures were used for fuel injection, there was not enough time for fuel to mix. Because the ignition delay was cut down, most of the fuel was burnt during the diffusion phase rather than the premixed mode, resulting in higher efficiency. When the crank angle rises, the rate of heat escape reduces, which may be proven by delaying the injection time in this manner. If the injection time is advanced beyond the maximum amount allowed, the cylinder pressure may be raised; nevertheless, this results in a slower pace at which heat is released from the engine.

The CO emission distribution is shown in Figure 7 in relation to the various injection timings. The delayed injection time reveals the point at which carbon monoxide (CO) production and emission are at their highest levels. This is because when the injection time is delayed, there is less time available for the fuel to undergo the required mixing and combustion processes. Hence, full combustion does not take place when the injector is delayed. As a direct result of this, there is an increase in the production of CO and its emissions.

The EINOx emission distribution is shown in Figure 8 in relation to the various injection timings. The delayed injection time reveals the point at which the EINOx production and emission are at their lowest levels. This is because when the injection time was delayed, there was less time available for the fuel to undergo the required mixing and combustion processes. Hence, full combustion did not take place when the injector was delayed. As a direct result, the proper pressure and temperature

buildup required to form EINOx were not reached. So, the amount of NOx emission reduces significantly with the retardation of injection timing.

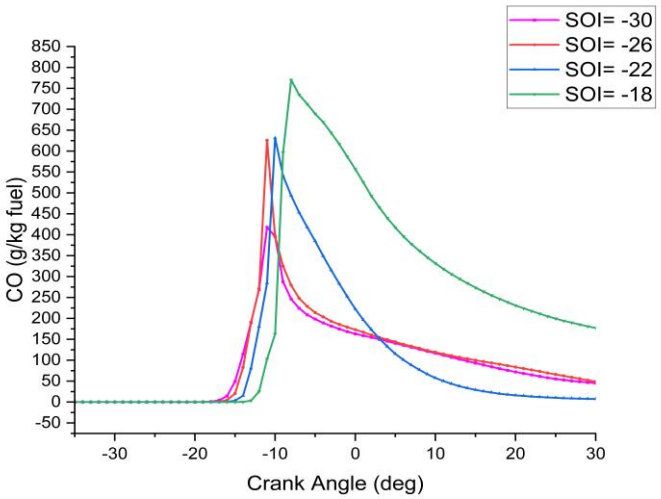

Fig. 7. CO Emission distribution for 40% butanol blends (CO vs CA)

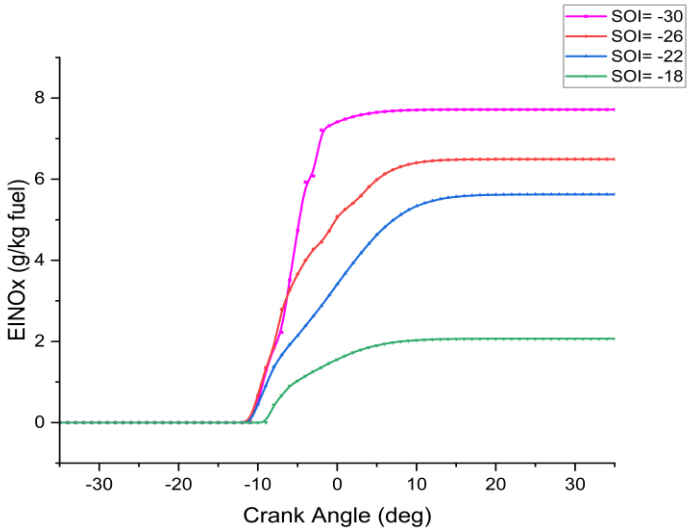

Fig. 8. Emission Indexed NOx (EINOx) distribution for 40% butanol blend (EINOx vs CA)

Since the delayed injection time did not allow for the appropriate mixing of fuel and air, the fuel mixture was not completely combusted. As a result, there was an increase in the total quantity of unburned hydrocarbon, as shown in Figure 9. At the point of discharge, the 18-degree BTDC indicates the maximum quantity of hydrocarbon that had not been consumed.

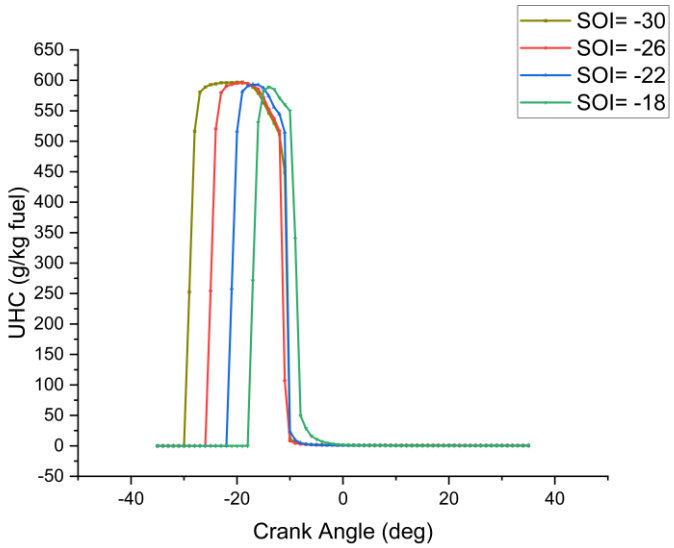

Fig. 9. Unburned Hydrocarbon distribution for 40% butanol blend (UHC vs CA)

3.2 Effect of Exhaust Gas Recirculation

Exhaust Gas Recirculation, often known as EGR, is a method for reducing the amount of nitrogen oxides (NOx) that includes introducing a part of the exhaust gas back into the intake air before delivering it to the engine's cylinder. As a result of this process, the amount of oxygen in the air was decreased, resulting in a lower rate of NOx production.

The impacts on the emission characteristics were investigated using D60B40 in conjunction with three different EGR percentages, including 10%, 20%, and 30%.

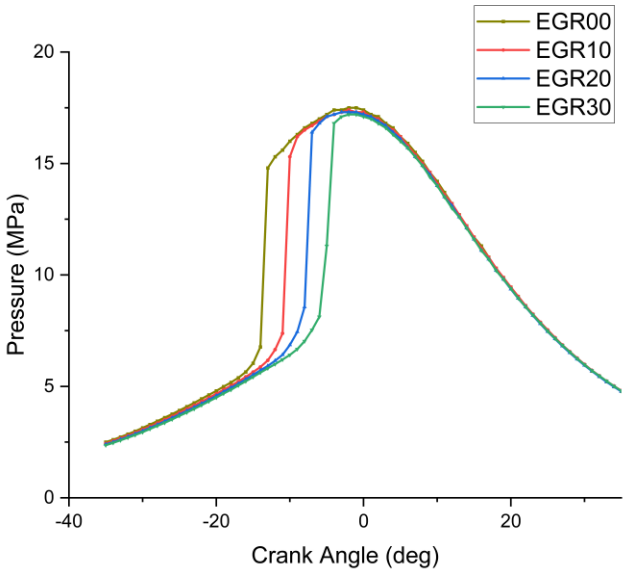

Fig.10. In-cylinder Pressure distribution for different EGR rates (Pressure vs CA)

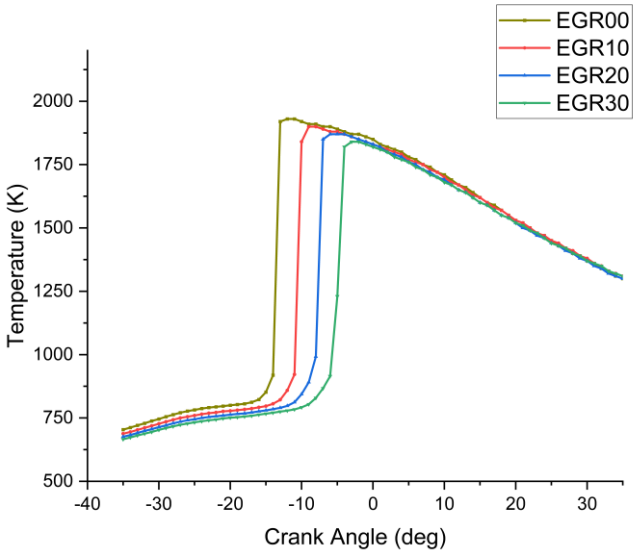

Fig. 11. Temperature distribution for different EGR rates (Temp. vs CA)

Figure 10 demonstrates that the pressure decreases when the amount of EGR in the system rises. The greatest pressure may be seen on the EGR00 gauge, which is the simple air intake. This is because a rise in the EGR rate reduced the quantity of fresh air, resulting in a lower concentration of oxygen in the air. Hence, the fuel mixture does not seem to have been completely combusted in this instance. Because of this, the pressure cannot rise to the desired amount, and instead it steadily decreases as the EGR rate increases.

Similar to the pressure distribution**,** Figure 11 shows the gradual decrease in the temperature with the increase of EGR percentage. A higher EGR rate means a larger portion of exhaust gas was being charged into the combustion chamber. With the shortage of oxygen concentration, complete combustion does not occur, so the peak temperature in the engine cylinder drops. As a consequence, the heat release rate also decreases.

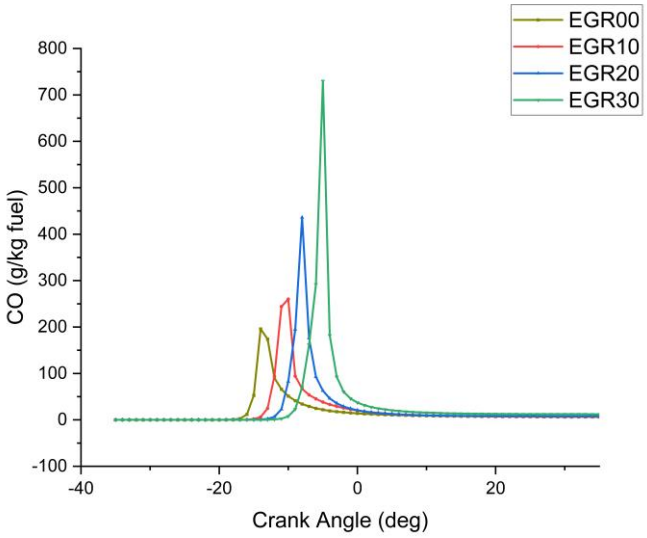

Fig. 12. CO Emission distribution for different EGR rates (CO. vs CA)

Since EGR decreased the quantity of oxygen in the combustion chamber, it caused an increase in the amount of carbon monoxide (CO) present in the exhaust stream. This is because a lower quantity of oxygen might induce incomplete combustion, which can lead to carbon monoxide (CO) production.

EGR's effect on a vehicle's CO emissions is variable and may be affected by various circumstances. By way of illustration, the use of EGR may bring about a decrease in the peak flame temperature that occurs during combustion. This, in turn, can promote more comprehensive combustion and reduce the production of CO.

Figure 12 shows the highest CO emission for 30% EGR, then gradually dropping for 20% and 10% EGR, which is quite similar to the 0% EGR.

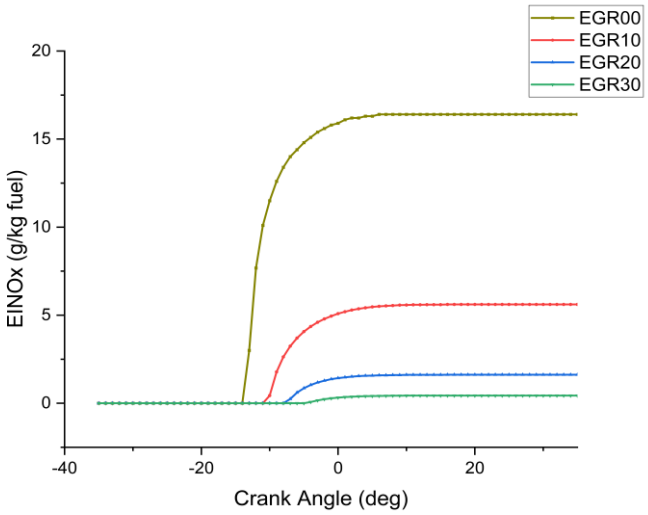

Fig. 13. Emission distribution EINOx for different EGR rates (EINOx vs CA)

Since EGR reduced the quantity of oxygen in the combustion chamber, the amount of nitrogen oxides produced in the exhaust was lowered, as shown in Figure 13. This is because a lower concentration of oxygen might result in combustion that is not complete. Hence, the pressure and temperature conditions necessary to produce NOx during the chemical reaction do not exist. As a consequence, the NOx levels in the intake air decreased when the rate of EGR is increased.

4. Conclusions

In this study, the effects of injection timing and the effect of exhaust gas recirculation were studied for a single-cylinder direct injection diesel engine fueled with 40% butanol and 60% diesel blend. The effects of injection timing were investigated for SOI= 18°, 22°, 26°, 30° BTDC. The EGR rates are set to 0%, 10%, 20% and 30% for the study. The research is concluded as follows:

i. Injection of fuel at an early stage, with an SOI of 30° BTDC, exhibits increased temperatures, pressures, and heat release rates.
ii. If early injection is used, the ignition delay will be longer, but the combustion length will be shorter. In the case of late injection, the situation is exactly the reverse.
iii. While early injection achieves superior results in reducing CO and unburned hydrocarbon, it increases NOx output. The late injection produces decreased NOx emission.

iv. The peak pressure and temperature decrease with the increase of the EGR rate. The lowest pressure was 16.7 MPa and 1771K, respectively, for EGR 30%.
v. CO emission increases for EGR by 10% but drops for EGR by 20% and 30%.
vi. The lowest NOx emission was recorded for EGR 30%, at 0.698 g/kg fuel.

Acknowledgment
The author wishes to express their heartfelt gratitude and thanks to the Department of Mechanical Engineering at KUET for all their assistance and support in effectively carrying out this simulation work.

References

[1] Mock, Peter, "CO_2 Emission Standards for Passenger Cars and Light-Commercial Vehicles in the European Union," The International Council on Clean Transportantion, Accessed July 10, 2024. https://theicct.org/publication/co2-emission-standards-for-passenger-cars-and-light-commercial-vehicles-in-the-european-union/
[2] Duan, Xiongbo, Jingping Liu, Yonghao Tan, Baojun Luo, Genmiao Guo, Zhenkuo Wu, Weiqiang Liu and Yangyang Li, "Influence of Single Injection and Two-Stagnation Injection Strategy on Thermodynamic Process and Performance of a Turbocharged Direct-Injection Spark-Ignition Engine Fuelled with Ethanol and Gasoline Blend," Applied Energy 228, (2018): 942-953. https://doi.org/10.1016/j.apenergy.2018.06.090
[3] Sadeghinezhad, E., S. N. Kazi, Foad Sadeghinejad, A. Badarudin, Mohammad Mehrali, Rad Sadri and Mohammad Reza Safaei, "A Comprehensive Literature Review of Bio-Fuel Performance in Internal Combustion Engine and Relevant Costs Involvement," Renewable and Sustainable Energy Reviews 30, (2014): 29-44. https://doi.org/10.1016/j.rser.2013.09.022
[4] Jin, Chao, Mingfa Yao, Haifeng Liu, F. Lee Chia-fon and Jing Ji, "Progress in the Production and Application of N-Butanol as a Biofuel," Renewable and Sustainable Energy Reviews 15, no. 8 (2011): 4080-4106. https://doi.org/10.1016/j.rser.2011.06.001
[5] Kumar, B. Rajesh and S. Saravanan, "Use of Higher Alcohol Biofuels in Diesel Engines: A Review," Renewable and Sustainable Energy Reviews 60, (2016): 84-115. https://doi.org/10.1016/j.rser.2016.01.085
[6] Othman, Mohd Fahmi, Abdullah Adam, G. Najafi and Rizalman Mamat, "Green Fuel as Alternative Fuel for Diesel Engine: A Review," Renewable and Sustainable Energy Reviews 80, (2017): 694-709. https://doi.org/10.1016/j.rser.2017.05.140
[7] Tipanluisa, Luis, Natalia Fonseca, Jesús Casanova and José-María López, "Effect of n-Butanol/Diesel Blends on Performance and Emissions of a Heavy-Duty Diesel Engine Tested Under the World Harmonised Steady-State Cycle," Fuel 302, (2021): 121204. https://doi.org/10.1016/j.fuel.2021.121204
[8] Gopinath, S., P. K. Devan, V. Sabarish, BV Sabharish Babu, S. Sakthivel and P. Vignesh, "Effect of Spray Characteristics Influences Combustion in DI Diesel Engine–A Review," Materials Today: Proceedings 33, (2020): 52-65. https://doi.org/10.1016/j.matpr.2020.03.130
[9] Mansor, Mohd Radzi Abu, Taib Iskandar Mohamad and Osama Sabah, "Numerical Investigation on Combustion and Emissions in a Direct Injection Compression Ignition Engine Fuelled with Various Hydrogen–Methane–Diesel Blends at Different Intake Air Temperatures," Energy Reports 7, (2021): 403-421. https://doi.org/10.1016/j.egyr.2021.07.110
[10] Raeie, Nader, Sajjad Emami and Omid Karimi Sadaghiyani, "Effects of Injection Timing, Before and After Top Dead Center on the Propulsion and Power in a Diesel Engine," Propulsion and Power Research 3, no. 2 (2014): 59-67. https://doi.org/10.1016/j.jppr.2014.06.001
[11] Yasin, Mohd Hafizil Mat, Rizalman Mamat, Ahmad Fitri Yusop, Daing Mohamad Nafiz Daing Idris, Talal Yusaf, Muhammad Rasul and Gholamhassan Najafi, "Study of a Diesel Engine Performance with Exhaust Gas Recirculation (EGR) System Fuelled with Palm Biodiesel," Energy Procedia 110, (2017): 26-31. https://doi.org/10.1016/j.egypro.2017.03.100

[12] O. P. Lopatin, "The Effect of Operational Modes of Diesel Engines to Emissions of Nitrogen Oxides," IOP Conference Series. Materials Science and Engineering 862, no. 6 (May 1, 2020): 062087. https://doi.org/10.1088/1757-899X/862/6/062087
[13] S. Saravanan, "Effect of Exhaust Gas Recirculation (EGR) on Performance and Emissions of a Constant Speed DI Diesel Engine Fueled with Pentanol/Diesel Blends," Fuel 160 (2015): 217-226. https://doi.org/10.1016/j.fuel.2015.07.089
[14] Deqing, Mei, Qian Junnan, Sun Ping, Miao Yan, Zhang Shuang and Cai Yongjun, "Study on the Combustion Process and Emissions of a Turbocharged Diesel Engine with EGR," Journal of Combustion 2012 (January 1, 2012): 1-9. https://doi.org/10.1155/2012/932724
[15] Emami, Sajjad and Samad Jafarmadar, "Multidimensional Modeling of the Effect of Fuel Injection Pressure on Temperature Distribution in Cylinder of a Turbocharged DI Diesel Engine," Propulsion and Power Research 2, no. 2 (2013): 162-175. https://doi.org/10.1016/j.jppr.2013.04.003
[16] Raeie, Nader, Sajjad Emami and Omid Karimi Sadaghiyani, "Effects of Injection Timing, Before and After Top Dead Center on the Propulsion and Power in a Diesel Engine," Propulsion and Power Research 3, no. 2 (2014): 59-67. https://doi.org/10.1016/j.jppr.2014.06.001
[17] De Albéniz Azqueta, Sergio Pérez, "ANSYS Forte Simulate Guide," Spain: Universidad Pública de Navarra, June 10, 2020, Accessed July 10, 2024. https://academica-e.unavarra.es/handle/2454/37481